1-1-1999

Determination of the Lithium Ion Diffusion Coefficient in Graphite

Ping Yu
University of South Carolina - Columbia

Branko N. Popov
University of South Carolina - Columbia, popov@engr.sc.edu

James A. Ritter
University of South Carolina - Columbia

Ralph E. White
University of South Carolina - Columbia, white@cec.sc.edu

Publication Info

Journal of the Electrochemical Society, 1999, pages 8-14.

Publisher's link: http://dx.doi.org/10.1149/1.1391556
DOI: 10.1149/1.1391556

Journal of The Electrochemical Society, **146** (1) 8-14 (1999)
S0013-4651(98)02-032-1 CCC: $7.00

Determination of the Lithium Ion Diffusion Coefficient in Graphite

Ping Yu,* B. N. Popov,,z J. A. Ritter,** and R. E. White****

Center for Electrochemical Engineering, Department of Chemical Engineering, University of South Carolina, Columbia, South Carolina 29208, USA

A complex impedance model for spherical particles was used to determine the lithium ion diffusion coefficient in graphite as a function of the state of charge (SOC) and temperature. The values obtained range from of 1.12×10^{-10} to 6.51×10^{-11} cm^2/s at 25°C for 0 and 30% SOC, respectively, and for 0% SOC, the value at 55°C was 1.35×10^{-10} cm^2/s. The conventional potentiostatic intermittent titration technique (PITT) and Warburg impedance approaches were also evaluated, and the advantages and disadvantages of these techniques were exposed.

Manuscript submitted February 6, 1998; revised manuscript received July 30, 1998.

The use of lithium-intercalated carbons as anodes instead of lithium metal for rechargeable lithium batteries helps in overcoming the severe degradation problems associated with the metallic lithium/solvent interface and the short cycle life due to dendrite formation during cycling. As alternative materials to replace lithium metal, graphite, pyrolytic carbon, mesophase carbon, carbon fiber, as well as carbons doped with P and N, have been studied extensively.[1-8] However, the lithium ion transport properties in these carbons have not been measured precisely due to experimental difficulties associated with the changes of lithium content with time during charging and discharging the electrode, and from uncertainties in the determination of the parameters necessary for evaluation of the lithium ion diffusion coefficient. These parameters include the dependence of the open-circuit potential of the anode upon the lithium content, the electrochemically active surface area, and the molar volume of the lithiated material.

Several electrochemical techniques have been developed to determine the diffusion coefficient of the lithium ion in carbon, such as potential intermittent titration technique (PITT), current pulse relaxation (CPR), potential step chronoamperometry (PSCA), cyclic voltammetry (CV), and electrochemical impedance spectroscopy (EIS). Reported values of the diffusion coefficient of the lithium ion in various carboneous materials[9-13] using these techniques vary greatly and are summarized in Table I. Note that the values reported by Takami et al.[12] are three orders larger than those given by Morita et al.[11]

The objective of this work was to determine the lithium ion diffusion coefficient in graphite. Here, the PITT, Warburg, and a complex faradaic impedance model for spherical particles were used to determine the lithium ion diffusion coefficient in graphite. The latter technique is an extension of the method reported by Motupally et al.[14] for determining the solid-state diffusion coefficient of protons in a nickel hydroxide film. Haran et al.[15] extended Motupally's planar diffusion model to spherical coordinates and used it to determine the diffusion coefficient of hydrogen in metal hydrides.

* Electrochemical Society Student Member.
** Electrochemical Society Member.
[a] E-mail: popov@engr.sc.edu

Theory

The graphite electrode considered here is a small, flat, cylindrical electrode that is filled with spherical graphite particles, as described in more detail in the Experimental section below. The electrode reaction at the surface of the graphite particle is[13]

$$\mathrm{Li}^+ + \mathrm{e}^- + S_c \underset{\text{discharge}}{\overset{\text{charge}}{\rightleftharpoons}} [\mathrm{Li}^{\vartheta} - S_c^{-\vartheta}] \qquad [1]$$

where S_c represents the vacant site within the graphite host and available for lithium intercalation. ϑ is the charge of lithium remaining after its intercalation. $-\vartheta$ is the charge the graphite host accumulates after lithium intercalation.[13] In this paper the charge process on graphite signifies the intercalation process of lithium into graphite, whereas the discharge process signifies lithium deintercalation from graphite.

PITT.—In PITT, the potentiostatic mode acts as a coulometer and the experimental parameters are charge vs. time. By assuming that the carbon particles are spherical, and by using the appropriate initial and boundary conditions, Fick's second law for a short-time approximation ($t \leq R^2/D$, where R is the maximum length of the diffusion path, i.e., the particle radius) leads to[9,16]

$$Q = \pm\frac{2FA\sqrt{D}}{\sqrt{\pi}}(C^0 - C_R)\sqrt{t} \quad (+ \text{ for discharge}, - \text{ for charge}) \qquad [2]$$

which describes the variation of charge with time. In Eq. 2, Q is the coulombs per unit mass of active material due to potentiostatic charging or discharging, t is the elapsed time from the beginning of the step, F is the Faraday constant, A is the effective surface area per unit mass of the electrode, D is the diffusion coefficient of Li^+, and C^0 and C_R are the concentrations of Li^+ before and after the voltage step, respectively. Thus, D is determined from the slope of a linear plot of Q vs. $\sqrt{t}$.

Warburg impedance.—This method was first proposed by Ho et al.,[17] where they expressed the Warburg impedance representing the diffusion of an ion as

Table I. Lithium ion diffusion coefficients in different carboneous materials.

Material	Diffusion coefficient (cm^2/s)	Range of x in Li_xC_6	Technique	Source
Petroleum coke	$1.0 \times 10^{-9} \sim 1.8 \times 10^{-8}$	$0 < x < 0.65$	PITT	Guyomard and Tarason[9]
Carbon fiber	$10^{-12} \sim 10^{-10}$	$0 < x < 0.6$	CPR and PSCA	Uchida et al.[10]
Pitch-based carbon fiber	$10^{-11} \sim 10^{-10}$	$0.1 < x < 0.5$	EIS	Morita et al.[11]
Carbon fiber	$10^{-7.7} \sim 10^{-6.4}$	$0.1 < x < 0.5$	EIS	Takami et al.[12]
Artificial graphite	$10^{-8.5} \sim 10^{-7.7}$	$0.1 < x < 0.5$	EIS	Takami et al.[12]
Carbon fiber	10^{-10}	$x = 0$	Modeling and CV	Verbrugge and Koch[13]

S1099-0062(98)02-032-1 CCC: $7.00

$$-Z_{Im} = \delta\omega^{-1/2} \text{ or } Z_{Re} = \delta\omega^{-1/2} \quad [3]$$

where

$$\delta = V_m(dE_{oc}/dx)/zFAm(2D)^{1/2} \text{ when } \omega >> D/R^2 \quad [3a]$$

and ω is the angular frequency, δ is the Warburg prefactor, V_m is the molar volume of lithiated material, (dE_{oc}/dx) is the gradient of the coulometric titration curve, which is obtained from a plot of the open-circuit potential vs. the composition "x" at each charged state, m is the amount of active material in the electrode, z is the charge number of the electroactive species, and z is equal to 1 for Li^+.

Modified EIS method.—According to Haran et al.,[15] the faradaic impedance of an electrochemical system is written as

$$Z(\omega) = \frac{\partial\eta_R}{\partial I} + \frac{(1-j)\sigma}{\sqrt{\omega}\left[\coth(1+j)\sqrt{\frac{\omega R^2}{2D}} - (1-j)\sqrt{\frac{D}{2\omega R^2}}\right]^{1/2}} \quad [4]$$

where η_R is the overpotential at $r = R$, I is the specific current due to the electrochemical reaction, j is the imaginary unit, $\sqrt{-1}$, and σ (modified Warburg prefactor) is expressed as[15]

$$\sigma = \frac{(\partial J/\partial C_R)}{(\partial J/\partial\eta_R)}\frac{m}{a_p V(1-\epsilon)F\sqrt{2D}} \quad [5]$$

where V is the volume of the cylindrical pellet electrode and a_p is the electroactive surface area per unit volume of the electrode. In Eq. 4, the faradaic impedance is a linear combination of the charge-transfer resistance and the diffusion impedance (modified Warburg) defined by the first and second terms on the right side of the equation, respectively. Separating the modified Warburg impedance into a real part (Z_{Re}) and an imaginary part (Z_{Im}) and differentiating Z_{Im} and Z_{Re}, gives the slope of the Nyquist plot in the diffusion-controlled region as[15]

$$\frac{d(Z_{Im})}{d(Z_{Re})} = \frac{T_4[-T_3 + (S_3S_5 + S_4S_7 - S_1S_6 + S_2S_8)\psi] - 2T_3(S_4S_3 + S_2S_1)\psi}{T_4[-T_5 + (S_3S_6 + S_4S_8 - S_1S_5 + S_2S_7)\psi] - 2T_5(S_4S_3 + S_2S_1)\psi} \quad [6]$$

$$T_3 = (S_4S_5 - S_2S_6): \quad T_4 = (S_4{}^2 + S_2{}^2): \quad T_5 = (S_4S_6 + S_2S_5) \quad [6a]$$

$$S_1 = S_5S_6: \quad S_2 = 2\psi - S_5: \quad S_3 = 2\coth(\psi)\cot(\psi)(1 - \psi S_6) - 2\psi S_5 + S_8 \quad [6b]$$

$$S_4 = 2\psi\coth(\psi)\cot(\psi) - S_6: \quad S_5 = \coth(\psi) - \cot(\psi) \quad [6c]$$

$$S_6 = \coth(\psi) + \cot(\psi): \quad S_7 = 2 - S_1: \quad S_8 = \coth(\psi)^2 + \cot(\psi)^2 \quad [6d]$$

$$\psi = \sqrt{\frac{\omega R^2}{2D}} \quad [6e]$$

Note that the ohmic resistance of the cylindrical electrode and the uncompensated solution resistance are not included in Eq. 4. Nevertheless, the ohmic resistance affects only the magnitude of the impedance, it has no effect on the slope of the Nyquist plot $[d(Z_{Im})/d(Z_{Re})]$ in the diffusion-controlled regime, which is the quantity being sought in this analysis. In addition, the double-layer capacitance is assumed to be negligible in the diffusion-controlled region, because the time constant for diffusion in a solid is much greater than the time constant corresponding to the double-layer capacitance.[14] Also, migration in the solid phase is neglected in this model because of the small charge carried by the Li ion.

Equations 6a-d are functions of ψ. According to Eq. 6e, ψ is defined in terms of the frequency, ω, diffusion coefficient, D, and the radius of the particle, R. Thus, with ω and R known, the diffusion coefficient of Li^+ is obtained from the slope of the Nyquist plot $[d(Z_{Im})/d(Z_{Re})]$ in the diffusion-controlled region.

Experimental

The electrochemical measurements were carried out using a Swagelock three-electrode cell (defined here as a T-cell) shown in Fig. 1. A typical graphite anode was prepared by mixing 16.3 mg of graphite powder (1-2 μm, Aldrich) with 10% polytetrafluoroethylene (PTFE, Aldrich) and roller pressed into a thin disk approximately 95 μm in thickness, 1.26 cm in diam, and 1.18×10^{-2} cm^3 in volume. The average value of 1.5 μm was used for the diameter of the graphite particle. The counter and reference electrodes were made of Li foil (99.9%, Aldrich), and a sheet of Whatman glass fiber membrane was used as the separator. The electrolyte consisted of 1 M $LiPF_6$ dissolved in a mixture of propylene carbonate (PC), ethylene carbonate (EC), and dimethyl carbonate (DMC) in a ratio of 1:1:3. The T-cell was assembled in a glove box filled with Ar. The cathode and anode separation was approximately 0.3 mm. After the cell was assembled, it remained in the glove box for 30 min to allow the electrolyte to disperse into the porous structure of the graphite anode prior to cycling and carrying out other electrochemical characterizations.

The reaction of Li with the organic electrolyte which results in the formation of the passivating film occurs during the first charge-discharge cycle. After two cycles, the passsive film formation rate decreases dramatically.[4,18] Thus, before carrying out the PITT and EIS measurements the T-cell was charged and discharged at least two cycles between 0 and 1.0 V vs. Li/Li^+ reference electrode using a constant current density of 0.1 mA/cm^2. The PITT was carried out potentiostatically at 0.2, 0.1, and 0.06 V vs. Li/Li^+ reference electrode. The state of charge (SOC) was estimated by the coulometric curve (Fig. 2) corresponding to these imposing potentials. In Fig. 2, $x = 0$ refers to 0% SOC, while $x = 1$ corresponds to 100% SOC. The impedance measurements were carried out on preconditioned electrodes. The fully charged electrodes were discharged for 2 h using the same current density of 0.1 mA/cm^2. Next the electrodes were allowed to stabilize at open-circuit potential, E_{oc}. The SOC was determined from the coulometric titration curve (Fig. 2) obtained for the stable open-circuit potential.

The experiments were carried out using Corrware and Zplot software version 1.4d (Scribner Associates, Inc.) with the EG&G Princeton Applied Research ac impedance system. The impedance tests covered the frequency range from 0.005 Hz to 10 kHz. The impedance experiments were carried out at 25 and 55°C and the PITT experiments only at 55°C.

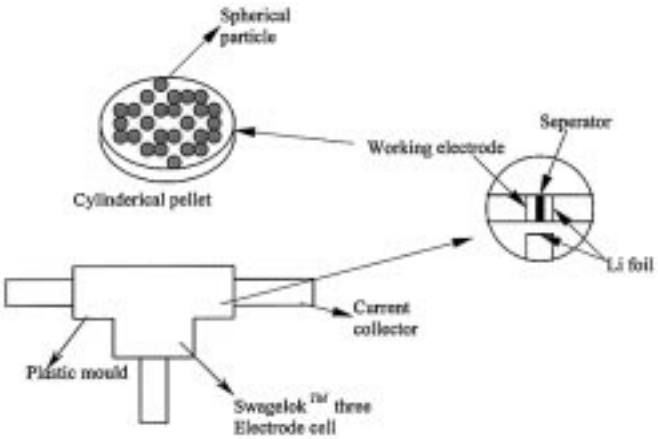

Figure 1. A schematic diagram of the Swagelock T-cell used in determining the Li^+ diffusion coefficient in graphite.

S1099-0062(98)02-032-1 CCC: $7.00

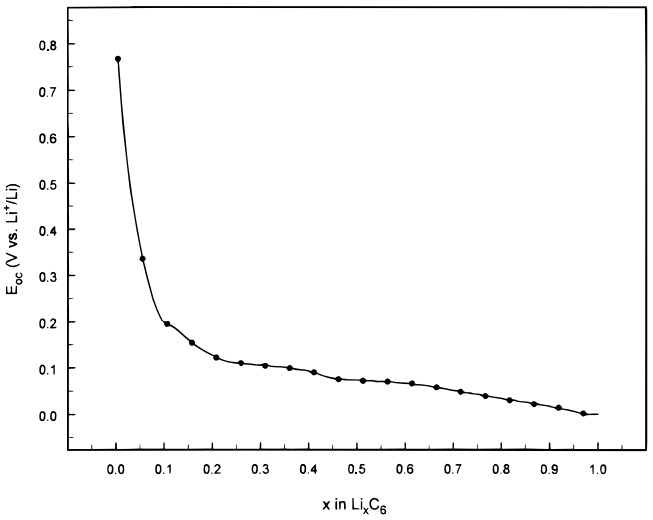

Figure 2. Coulometric titration curve for graphite.

Results and Discussion

Determination of the Li^+ diffusion coefficient using PITT.—As shown in Eq. 2, the value of the diffusion coefficient can be extracted from the slope of a Q vs. $\sqrt{t}$ plot with known values of A, C^o, and C_R. The values of C^o and C_R were obtained in this work as follows: the compositions "x" (in Li_xC_6) before and after a voltage step were obtained from the coulometric titration curve (dependence of the open-circuit potential, E_{oc}, vs. composition "x"). Next, the C^o or C_R value was estimated using Eq. 7

$$C = \frac{(x/6)}{12\ \text{g/mol}} \times 2.0\ \text{g/cm}^3 \qquad [7]$$

where 12 g/mol is the molecular weight of carbon, 2.0 g/cm^3 [19] is the density of carbon, and x/6 is the molar ratio of lithium to carbon in Li_xC_6. For example, the composition x was determined to be 0.09 (i.e., 9% SOC) from the coulometric titration curve (Fig. 2) when the graphite electrode was charged at 0.2 V vs. Li/Li^+, then the concentration C_R was calculated to be 2.5×10^{-3} mol/cm^3 according to Eq. 7. The effective surface area, A, was determined by a Brunauer-Emmett-Teller (BET) measurement using a Micrometrics Pulse Chemisorb 2700. The value of A here is 1.5 m^2/g.

The potentiostatic intermittent titration curves for graphite at various SOCs are given in Fig. 3. The integration of current J vs. time in Fig. 3 gives the values of the charging coulumbs Q. Figure 4 shows the corresponding dependence of Q on $t^{1/2}$ for different SOCs, which all appear to be quite linear. The slope of Q vs. $t^{1/2}$ at 9% SOC is 6.01 C/g s$^{0.5}$. With the initial concentration C^o of zero, the concentration C_R of Li^+ equal to 2.5×10^{-3} mol/cm^3 after the potential of 0.2 V vs. Li/Li^+ was imposed, and the effective surface area at 1.5 m^2/g, the Li^+ diffusion coefficient was calculated from Eq. 2 to be 1.03×10^{-12} cm^2/s. Figure 5 shows that the diffusion coefficients determined using the PITT technique ranged of 1.03×10^{-12} to 9.30×10^{-14} cm^2/s, and that they decreased with an increase in SOC from 9 to 57%.

Determination of the Li^+ diffusion coefficient by the EIS method using Warburg impedance.—The electrochemical impedance spectra obtained for graphite at various SOCs are shown in Fig. 6. The frequencies in the diffusion-controlled region and the charge-transfer region are also indicated in Fig. 6. The Warburg impedance Z_{Im} in the diffusion-controlled region is plotted in Fig. 7 as a function of $\omega^{-1/2}$ at different SOCs. A linear relationship of Z_{Im} vs. $\omega^{-1/2}$ was observed for graphite at each SOC. In Eq. 3a, the value of V_m was calculated to be 8.69 cm^3/mol with the electrode volume of 1.18×10^{-2} cm^3, the electrode mass of 16.3 mg, and the formula weight of 12 g/mol for carbon. At 35% SOC ($x = 0.35$ in Li_xC_6), the value of dE_{oc}/dx was determined to be 0.8159 from the coulomb titration curve in Fig. 2

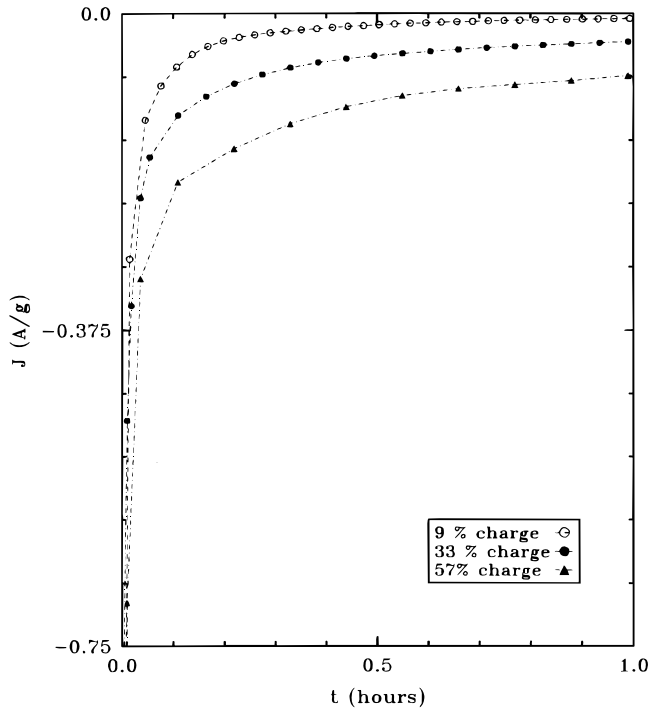

Figure 3. Potentiostatic intermittent titration curves for graphite at various SOCs; $T = 55$°C.

and the slope of Z_{Im} vs. $\omega^{-1/2}$ was 0.4553 from Fig. 7; the corresponding Li^+ diffusion coefficient in graphite was then estimated to be 2.27×10^{-13} cm^2/s. The values of diffusion coefficient at different states of charge are plotted in Fig. 5 along with the PITT results.

Determination of the Li^+ diffusion coefficient by the modified EIS method.—To compare the results obtained using the conventional

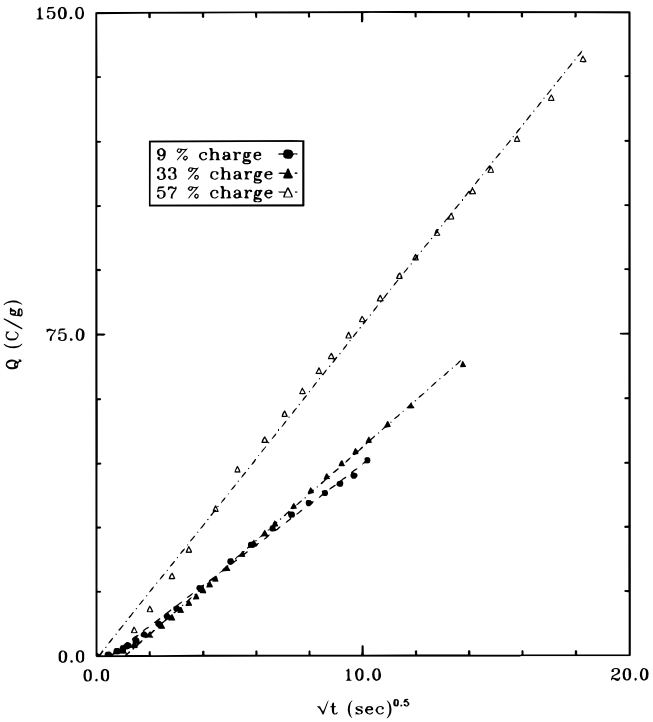

Figure 4. Q as a function of $t^{1/2}$ for graphite at various SOCs extracted from Fig. 3; T = 55°C.

S1099-0062(98)02-032-1 CCC: $7.00

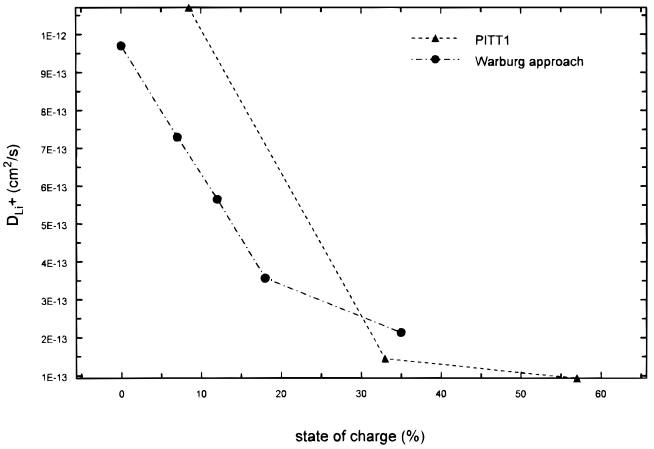

Figure 5. Li^+ diffusion coefficients as a function of the SOC determined by PITT and Warburg impedance approaches; $T = 55°C$.

Warburg approach with those estimated using the modified EIS model,[15] simulations were carried out for different Li^+ diffusion coefficients. These simulations were performed with the values of frequency, ω, ranging from 0.01 to 100 Hz, the graphite particle spherical radius of 0.75 μm, the Warburg prefactor, σ, of 5 $\Omega/s^{1/2}$ and $\partial\eta_R/\partial I$ of 10 Ω (the values of σ and $\partial\eta_R/\partial I$ were arbitrarily chosen). The results are shown in Fig. 8. The modified impedance is characterized by three distinct regions: the semi-infinite, transition, and finite diffusion regions.[14,20-22] The frequency range corresponding to these regions is related to the value of the diffusion coefficient and to the radius of the particle. At high frequencies, when $\omega << D/R^2$, the hyperbolic cotangent term tends to unity in Eq. 4. As a result, the modified Warburg impedance simplifies to the conventional Warburg impedance. In such a case, a straight line with an angle of 45°, corresponding to the semi-infinite diffusion region, is observed in the Nyquist plot (Fig. 8). At lower frequencies, when $\omega >> D/R^2$, the slope of the imaginary vs. real plot approaches infinity, and, i.e., as shown in Fig. 8, a vertical line perpendicular to the real-axis is seen on a Nyquist plot, corresponding to the finite diffusion region. The transition region,[14,20-22] at which the angular frequency is close to the value of D/R^2, lies between the semi-infinite and finite diffusion regions. In Fig. 8, each of the three characteristic regions is easily identified, where it is seen that increasing the diffusion coefficient increases the abscissa value for the onset of the transition region.

During the simulations the values of σ = 5 $\Omega/s^{1/2}$ and $(\partial\eta_R/\partial I)$ = 10 Ω were used as known parameters. Note that these parameters affect only the magnitude of the impedance; they have no effect on

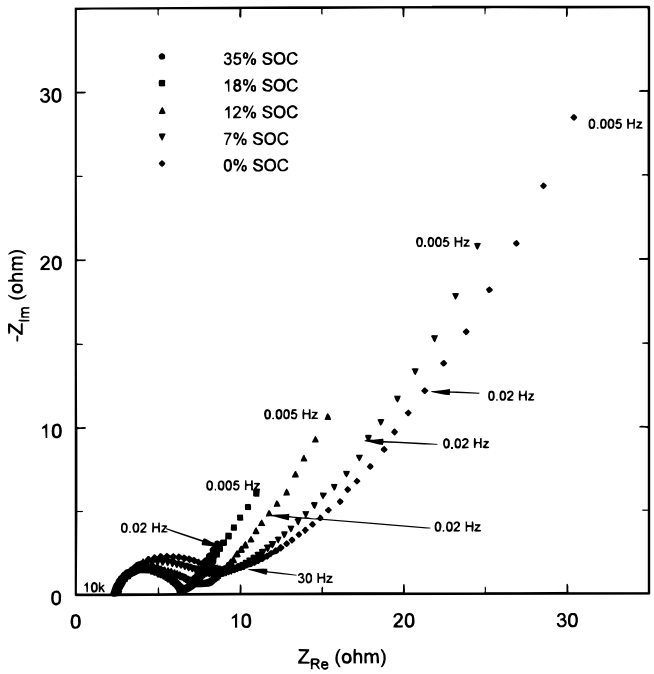

Figure 6. Nyquist plots for graphite at various SOCs and at 55°C.

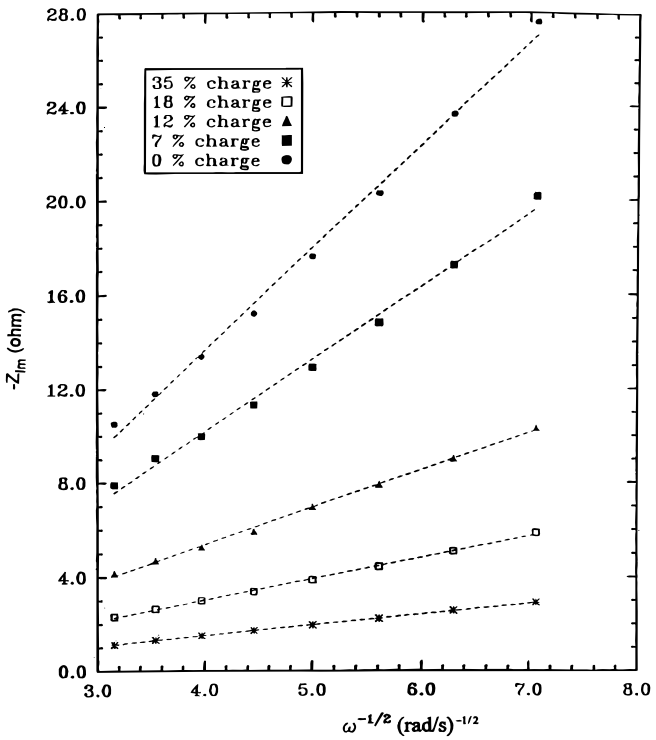

Figure 7. Warburg impedance, Z_{Im}, as a function of $\omega^{-1/2}$ for graphite at various SOCs exacted from Fig. 6.

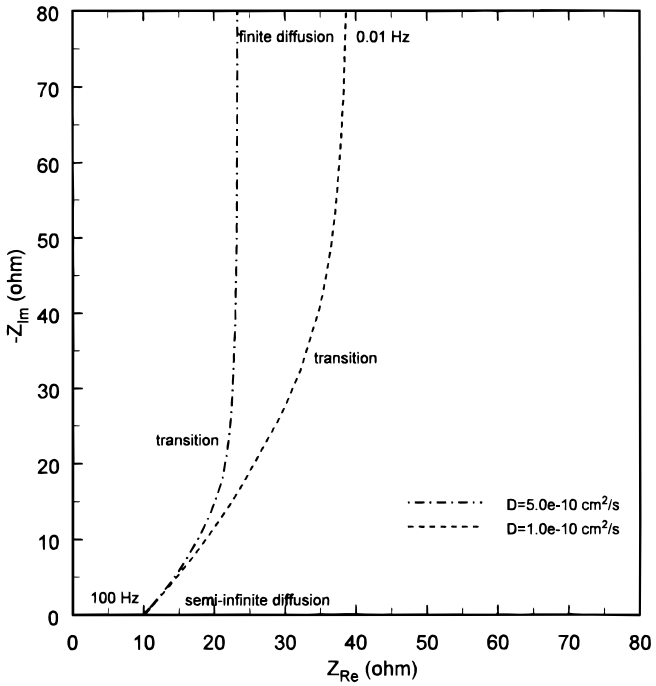

Figure 8. Simulation results from the modified EIS model with different lithium ion diffusion coefficients. The values of σ and $(\partial\eta_R/\partial I)$ were set to 5 $\Omega/s^{1/2}$ and 10 Ω, respectively.

S1099-0062(98)02-032-1 CCC: $7.00

the slope of the Nyquist plot in the diffusion-controlled regions. So their magnitudes were not critical to the foregoing analysis.

The method for extracting the diffusion coefficient from the transition region is well exploited in literature.[14,20-24] Mathias and Haas[22] used the equation[20] $D = L^2\omega/5.12$ to calculate the diffusion coefficient with the slope of -2.0 in the transition region. Pyun[23] employed the equation[24] $D = \pi f R^2/1.94$ (where f is the frequency at the transition region) to obtain the diffusion coefficient. In their work, only a single slope or single frequency in the transition region was used for determining the diffusion coefficient, which can lead to an error because the transition region cannot be specified exactly with only one data point in a Nyquist plot. Similar to Motupally et al.,[14] the frequencies for the slopes in the range of -1.5 to -2.5 (between 0.005 and 0.02 Hz) were considered in this work to correspond to the transition region, and were used for determining the diffusion coefficients.

The impedance data presented in Fig. 6 were reprocessed by using the modified EIS model. The transition regions at different SOCs are shown in Fig. 9. The Li^+ diffusion coefficient at each SOC was determined using the following procedure. The imaginary and real parts of the EIS data at each state of charge in the diffusion region were fitted to a polynomial function of the form

$$Z_{Im} = a + bZ_{Re} + cZ_{Re}^2 \quad [8]$$

The fitting parameters a, b, and c were then determined. A slope was obtained by differentiating the polynomial function at each data point. Next, Eq. 6a-e were solved for ψ at each frequency in the transition region with the slopes between -1.5 and -2.5. The Li^+ diffusion coefficients were estimated using Eq. 6e for the known frequency and radius of the spherical graphite particle (0.75 μm). For example, Eq. 8 fitted to the data at 0% SOC (fully discharged state) resulted in $Z_{Im} = 0.1311 - 0.1204Z_{Re} + 0.0363Z_{Re}^2$. By taking the slope of this function at each data point and solving Eq. 6a-d, the values of the Li^+ diffusion coefficient at each data point were determined. These values were averaged to obtain $D = 1.35 \times 10^{-10}$ cm^2/s for 0% SOC. The same procedure was repeated at other states of charge.

Figure 10 shows the EIS data and Eq. 8 correlations at 25 and 55°C and at 0% SOC. The slopes in the transition region varied with temperature. The values of the Li^+ diffusion coefficients estimated

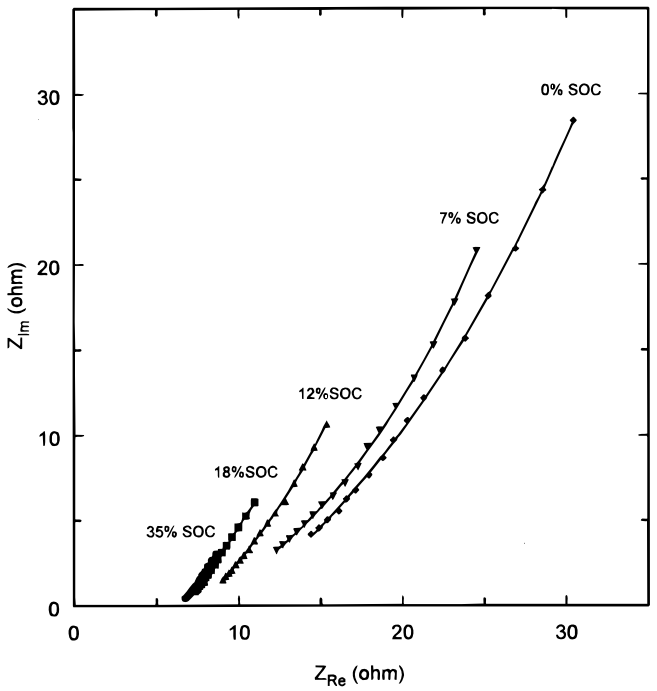

Figure 9. Nyquist plots in the diffusion region for graphite at various SOC at 55°C. Solid symbols are experimental data and lines are fitted equations.

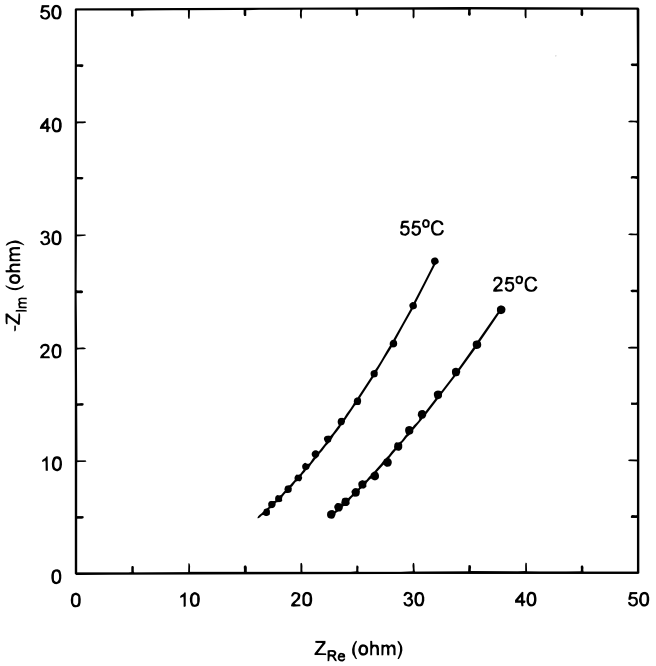

Figure 10. Nyquist plots in the diffusion region for the diffusion of Li^+ graphite at 0% SOC, and at 25 and 55°C. Solid symbols are experimental data and lines are fitted equations.

at the two different temperatures and at various SOCs are presented in Fig. 11. It is seen that increasing the SOC from 0 to 30% caused the Li^+ diffusion coefficient at 25°C to decrease only slightly from 1.12×10^{-10} to 6.51×10^{-11} cm^2/s. These values are in good agreement with those estimated by Morita et al.[11] and Verbrugge and Koch.[13] The Li^+ diffusion coefficients at 55°C also decreased only slightly by increasing the SOC, and the Li^+ diffusion increased slightly with increasing temperature. At 0% SOC, the Li^+ diffusion coefficients at 25 and 55°C were 1.12×10^{-10} and 1.35×10^{-10} cm^2/s, respectively. The value of the activation energy at 0% SOC was estimated from these values using an Arrhenius expression to be 5.1 kJ/mol, which is in agreement with that reported in the literature (7.5 kJ/mol for Li^+ diffusion in a LiAl alloy).[1,9]

The diffusion and migration through the passivating film were not accounted for in this model. This was because the transition frequency region analyzed in this study was far from the frequency region where the passivating film is active. The frequencies in the transition region used to determine the Li^+ diffusion coefficient and

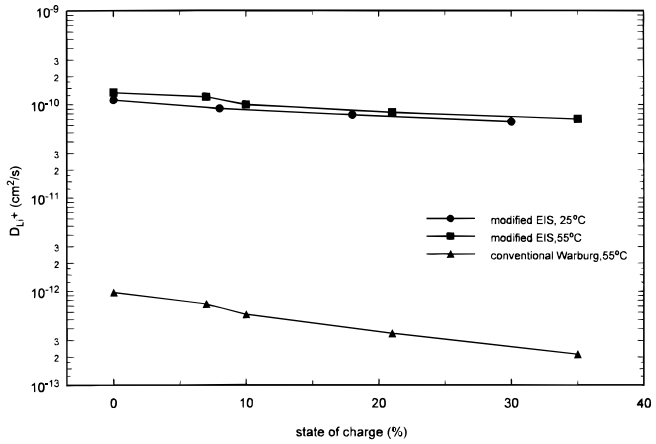

Figure 11. Li^+ ion diffusion coefficients in graphite determined by the modified EIS method as a function of the SOC at various temperatures; the values obtained from the Warburg method are presented for comparison.

S1099-0062(98)02-032-1 CCC: $7.00

the frequencies in the region associated with the diffusion process in a porous passivation film at 0% SOC are shown in Fig. 12. The slopes recorded in the frequency region between 1.58 to 30 Hz were determined to be 0.49 ~ 0.38 with a phase angle of approximately 22°. Takami et al.[12] suggested that this part of the curve is associated with diffusing of lithium ions through a porous passivating film. The porous structure of the passivating film was also confirmed by Liu and Wu.[25] As shown in Fig. 12, the frequencies used in this study for determining the Li^+ diffusion coefficient fell between 0.005 and 0.02 Hz resulting in slopes of −1.5 to −2.5, indicating that by using this complex model one estimates only the diffusion coefficient in bare graphite.

Comparison of the different methods used to estimate the Li^+ diffusion coefficients.—According to this study, the diffusion coefficients obtained using the PITT and Warburg impedance techniques were two orders of magnitude smaller than those obtained using the modified EIS approach, and their dependence on the SOC was much less in the latter technique. The observed differences in the values obtained for the Li^+ diffusion coefficients were due to inaccuracies of the PITT and Warburg techniques. The accuracy of the PITT method for determining the Li^+ diffusion coefficient in graphite depends on accurate estimations of C^o, C_R, and A. Similarly, the precision of the Warburg impedance approach depends on accurate estimations of V_m, (dE_{oc}/dx), and A. Graphitized carbon typically shows several voltage plateaus in the open-circuit voltage, E_{oc}, vs. "x" profile due to a staging phenomenon[26] (as shown in Fig. 2), which impedes accurate determinations of (dE_{oc}/dx), C^0, and C_R. In addition, because the value of V_m depends upon the degree of graphitization,[12] the molar volume of lithiated material must be determined from the stoichiometry of the Li intercalation reaction into various carbons. Estimation of V_m using only the initial state of the carbon does not yield very accurate values.[10,11] Moreover, although the specific surface area can be measured using the BET single-point method, the electrochemically active surface area is always smaller than the physical surface area. Thus, problems associated with obtaining accurate values of (dE_{oc}/dx), C^o or C_R, A, and V_m limit the application of the PITT and Warburg impedance approaches for determining Li^+ diffusion coefficients in carbon particles. Also, the Warburg impedance technique applies only to systems that are exactly in the semi-infinite diffusion-controlled region, where the slope of Z_{Im} vs. Z_{Re} is equal to 1. In fact, application of the Warburg impedance technique over the entire diffusion region, where slopes other than −1 exist, produces erroneous values of the Li^+ diffusion coefficient.

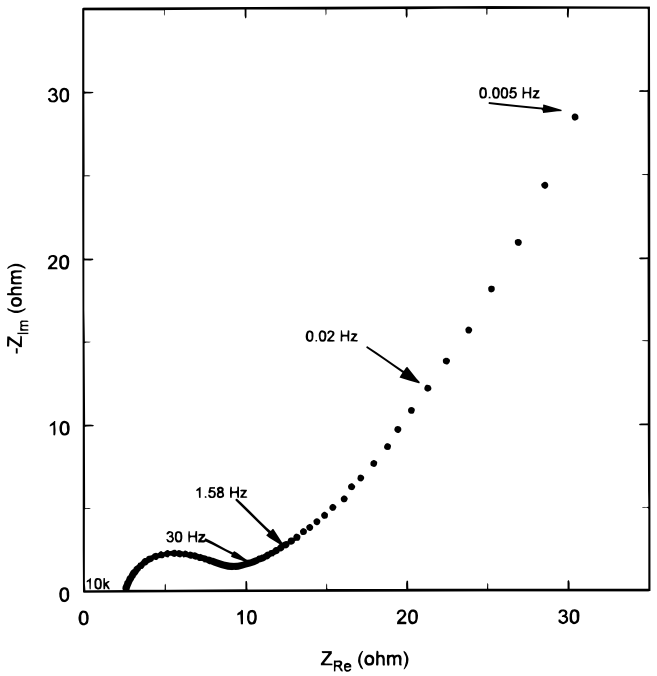

Figure 12. Nyquist plots for graphite at 0% SOC at 55°C.

The modified impedance approach presented here for determining the Li^+ diffusion coefficient in spherical carbon particles is based on determining only the slope of Z_{Im} vs. Z_{Re} in the transition region. The slope in the transition diffusion region is only a function of ψ, which according to Eq. 6e, is defined solely in terms of ω, D, and R. Thus, with known values of ω and R, the Li^+ diffusion coefficient in spherical carbon particles can be obtained from the slope in the transition diffusion region with much higher accuracy compared to the PITT or conventional Warburg impedance approaches.

Conclusions

An impedance model for a spherical particle was used to determine the Li^+ diffusion coefficient in graphite from EIS data as a function of SOC and temperature. The Li^+ diffusion coefficient values were found to depend only weakly on the SOC of the electrode. The Li^+ diffusion coefficients obtained for 0 and 30% SOC at 25°C were 1.12×10^{-10} and 6.51×10^{-11} cm^2/s, respectively, which is in agreement with results reported in the literature.[11,13] Slightly higher Li^+ diffusion coefficients were found at 55°C. At 0% SOC, the values of the Li^+ diffusion coefficients at 25 and 55°C were 1.12×10^{-10} and 1.35×10^{-10} cm^2/s, respectively. The corresponding activation energy was estimated to be 5.1 kJ/mol, also in agreement with that reported in the literature.[16]

The conventional electrochemical methods, i.e., the PITT and Warburg impedance approaches were evaluated for determining the Li^+ diffusion coefficient in graphite. The Li^+ diffusion coefficients estimated using the PITT and Warburg impedance methods were two orders of magnitude lower than those obtained using the modified EIS approach and the dependence on the SOC was much less in the latter technique. The observed differences in the Li^+ diffusion coefficients resulted from uncertainties in the estimations of the parameters that were required in the PITT and Warburg impedance approaches, such as (dE_{oc}/dx), C^o and C_R, V_m, and A. In contrast, only ω and R are required in the modified EIS method, which gave rise to less uncertainty compared to the PITT and conventional Warburg impedance approaches in estimating the Li^+ diffusion coefficient in carbon materials.

Acknowledgments

This material is based upon work supported in part by the DOE Division of Chemical Sciences, Office of Basic Energy Sciences, G. M. De-FG02-96ER 146598, and in part by the Office of Research and Development, CIA C/O No. 93-FI48100-100.

The University of South Carolina assisted in meeting the publication costs of this article.

List of Symbols

a_p	surface area per unit volume, cm^2/cm^3
A	effective surface area per unit mass of the electrode, cm^2/g
C	concentration of Li^+ in the negative electrode, mol/cm^3
C^o	initial Li^+ concentration, mol/cm^3
C_R	concentration of Li^+ at the particle surface ($r = R$), mol/cm^3
D	diffusion coefficient of Li^+ in the particle, cm^2/s
E_{oc}	open-circuit potential, V
f	frequency in the transition region, Hz
F	Faraday's constant, 96,487 C/equiv
I	current due to the electrochemical reaction, A
j	imaginary number, $\sqrt{-1}$
J	specific current per unit mass of active material, A/g
L	film thickness, cm
m	amount of active material, g
Q	charge per unit mass of active material, C/g
r	radial coordinate, cm
R	radius of spherical particle, cm
SOC	state of charge, between 0 and 100%
t	time, s
V	volume, cm^3
V_m	molar volume of lithiated material, cm^3/mol
x	stoichiometric parameter in Li_xC_6, mol
z	charge number of the electroactive species, equal to 1 for Li^+

S1099-0062(98)02-032-1 CCC: $7.00

Z	impedance, Ω
Z_{Im}	imaginary impedance, Ω
Z_{Re}	real impedance, Ω

Greek

ϵ	porosity of the electrode
σ	modified Warburg prefactor defined in Eq. 5, $\Omega/s^{1/2}$
δ	Warburg prefactor defined in Eq. 4, $\Omega/s^{1/2}$
ϑ	charge number of lithium remaining after its intercalation
ω	angular frequency, rad/s
η	overpotential, V
η_R	overpotential at the particle surface ($r = R$), V
ψ	defined by Eq. 6e
$\partial\eta_R/\partial I$	charge-transfer resistance, Ω

References

1. K. Tokumitsu, A. Mabuchi, H. Fujimoto, and T. Kasuh, *J. Power Sources*, **54**, 444 (1995).
2. M. Ishikawa, T. Nakamura, M. Morita, Y. Matsuda, S. Tsujioka, and T. Kawashima, *J. Power Sources*, **55**, 127 (1995).
3. W. J. Weydanz, B. M. Way, T. van Buuren, and J. R. Dahn, *J. Electrochem. Soc.*, **141**, 900 (1994).
4. A. M. Christie and C. A. Vincent, *J. Appl. Electrochem.*, **26**, 255 (1996).
5. H. Shi, J. Barker, M. Y. Saidi, and R. Koksbang, *J. Electrochem. Soc.*, **143**, 3466 (1996).
6. J. R. Dahn, R. Fong, and M. J. Spoon, *Phys. Rev. B*, **42**, 6424 (1990).
7. R. Yazami and M. Deschamps, *Bull. Electrochem.*, **12**, 206 (1996).
8. T. D. Tran, J. H. Feikert, X. Song, and K. Kinoshita, *J. Electrochem. Soc.*, **142**, 3297 (1995).
9. D. Guyomard and J. M. Tarascon, *J. Electrochem. Soc.*, **139**, 937 (1992).
10. T. Uchida, Y. Morikawa, H. Ikuta, and M. Wakihara, *J. Electrochem. Soc.*, **143**, 2606 (1996).
11. M. Morita, N. Nishimura, and Y. Matsuda, *Electrochim. Acta*, **38**, 1721 (1993).
12. N. Takami, A. Satoh, M. Hara, and T. Ohsaki, *J. Electrochem. Soc.*, **142**, 371 (1995).
13. M. W. Verbrugge and B. J. Koch, *J. Electrochem. Soc.*, **143**, 600 (1996).
14. S. Motupally, C. C. Streinz, and J. W. Weidner, *J. Electrochem. Soc.*, **142**, 1401 (1995).
15. B. Haran, B. N. Popov, and R. E. White, *J. Power Sources* (1998).
16. C. J. Wen, B. A. Boukamp, R. A. Huggins, and W. Weppner, *J. Electrochem. Soc.*, **126**, 2258 (1979).
17. C. Ho, I. D. Raistrick, and R. A. Huggins, *J. Electrochem. Soc.*, **127**, 343 (1980).
18. D. Aurbach, Y. Ein-Eli, and O. Chusid, *J. Electrochem. Soc.*, **141**, 603 (1994).
19. *Handbook of Chemistry and Physics*, R. C. Weast, Editor, 52nd ed., Chemical Rubber Co., Cleveland, OH (1972).
20. R. D. Armstrong, *J. Electroanal. Chem.*, **198**, 177 (1986).
21. R. D. Armstrong, B. Lindhom, and M. Sharp, *J. Electroanal. Chem.*, **202**, 69 (1986).
22. M. F. Mathias and O. Haas, *J. Phys. Chem*., **96**, 3174 (1992).
23. S. Pyun and J. Bae, *Electrochim. Acta*, **41**, 919 (1996).
24. R. Cabanel, G. Barral, J.-P. Diard, B. Le Gorrec, and C. Montella, *J. Appl. Electrochem*., **23**, 93 (1993).
25. P. Liu and H. Wu, *J. Power Sources*, **99**, 55 (1995).
26. J. R. Dahn, R. Fong, and M. J. Spoon, *Phys. Rev. B*, **42**, 6424 (1990).